

Submillimeter/millimeter observations of the molecular clouds associated with the Tycho' Supernova Remnant

Jin-Long Xu,^{1,2,3} Jun-Jie Wang^{1,2} and Martin Miller⁴

¹ National Astronomical Observatories, Chinese Academy of Sciences, Beijing 100012, China; xujl@bao.ac.cn

² NAOC-TU Joint Center for Astrophysics, Lhasa 850000, China

³ Graduate University of the Chinese Academy of Sciences, Beijing, 100080, China

⁴ I.Institute of Physics, University of Cologne, Cologne, 50937, Germany

Received 2010 September 16; accepted 2010 December 10

Abstract We have carried out CO $J = 2 - 1$ and CO $J = 3 - 2$ observations toward Tycho's supernova remnant (SNR) using the KOSMA 3m-Telescope. From these observations we identified three molecular clouds (MCs) around the SNR. The small cloud in the southwest was discovered for the first time. In the north and east, two MCs (cloud A and cloud B) adjacent in space display a bow-shaped morphology, and have broad emission lines, which provide some direct evidences of the SNR-MCs interaction. The MCs is revealed at $-69 \sim -59 \text{ km s}^{-1}$, well coincident with the Tycho's SNR. The MCs associated with Tycho's SNR have a mass of $\sim 2.13 \times 10^3 M_{\odot}$. Position-velocity diagrams show the two clouds adjacent in velocity which means possible cloud-cloud collision in this region. The maximum value (0.66 ± 0.10) of integrated CO line intensity ratio ($I_{\text{CO},J=3-2}/I_{\text{CO},J=2-1}$) for the three MCs agrees well with the previous measurement of individual Galactic MCs, implying that the SNR shock just drove into the MCs. The two MCs have a line intensity ratio gradient. The distribution of the ratio appears to indicate that the shock propagates from the southwest to the northeast.

Key words: ISM: individual objects (Tycho's Supernova Remnant (G120.1+1.4)) – ISM: molecules – supernova remnants

1 INTRODUCTION

When a supernova explodes near the molecular clouds (MCs), shock generated by supernova remnant (SNR) can accelerate, compress, heat or even fragment surrounding interstellar MCs. They also can enhance abundances with respect to quiescent cloud conditions of different molecular species. So the SNR-MCs interaction plays a very important role in the evolution of Interstellar Medium (Reynoso et al. 2000). Moreover, the molecular lines observations of MCs adjacent to SNRs can shed light on the SNRs' dynamical evolution and physical properties. So far about half of the Galactic SNRs are expected to be in physical associated with MCs (Reynoso & Mangum 2001). The association is indicated by morphological correspondence of molecular emission, presence of molecular line broadening within the extent of SNR, and presence of line emission with high high-to-low excitation line intensity ratio, etc (see Jiang et al. 2010). However, only few cases about the SNR-MCs interaction has been well confirmed. Even for some SNRs interacted with the surrounding MCs, the detailed distribution of environmental molecular gas is poorly known.

Tycho's SNR is known as a young type Ia SNR located in the Perseus arm (Albinson et al. 1986), with an age of about 400 years. The distance of Tycho's SNR is estimated to be 2.3 kpc (Kamper et al. 1978; Albinson et al. 1986; Strom 1988). The remnant has been widely studied in various wavebands. From the neutral hydrogen HI observation, Schwarz et al. (1995) concluded that the distance should be 4.6 ± 0.5 kpc; Reynoso et al. (1999) have performed an HI absorption study toward the remnant, suggesting that Tycho's SNR is currently interacting with a dense HI concentration in the northeast ($V_{LSR} = -51.5 \text{ km s}^{-1}$), which locally slows down the expansion of the shock front. In radio continuum (Reynoso et al. 1997) and high-resolution X-ray wavebands (Hwang et al. 2002), they indicated that the radio continuum and X-ray emission along the northeastern edge of Tycho's SNR is strongest. Based on the VLA observation, Dickel et al. (1991) indicates that the northeastern edge of Tycho's SNR is expanding with a very small and decreasing velocity into the dense interstellar medium, and may interact with it. Lee & Koo (2004) made the CO $J = 1 - 0$ line observation towards Tycho's SNR. They concluded that most of the CO $J = 1 - 0$ emission around Tycho's SNR is between -67 and -60 km s^{-1} , but the velocity component in intervals $-63.5 \sim -61.5 \text{ km s}^{-1}$ appears to be in contact with the Tycho's SNR along its the northeast boundary. Using CO $J = 1 - 0$ line to study the environs of Tycho's SNR, Cai et al. (2009) found that the CO $J = 1 - 0$ emission form a semi-closed molecular shell around the SNR, the emission in velocity range of $-69 \sim -58 \text{ km s}^{-1}$ is associated with the SNR. Because the calculated virial mass of clumps is greater than their gravitational mass, they suggested that CO molecular clumps are being violently disturbed by Tycho's SNR shock.

In order to understand the evolution of SNR interacting with MCs and investigate the detailed distribution of the molecular gas around Tycho's SNR, we have performed CO $J = 2 - 1$ and CO $J = 3 - 2$ observation toward Tycho' SNR. The observations cover for the first time the whole area of Tycho's SNR in these frequencies. Due to the observed molecular lines at higher frequencies, we can attain higher angular resolution, which is critical to identify relatively compact core. Also, higher J transitions are relatively more sensitive to hot gas. Thus, we can detailedly understand the distribution of the molecular gas in the vicinity of Tycho's SNR.

2 OBSERVATIONS

The observations of Tycho' SNR were made in CO $J = 2 - 1$ and CO $J = 3 - 2$ lines using the 3m KOSMA sub-millimeter telescope at Gornergrat, Switzerland in Jan, 2004. The half-power beam widths of the telescope at observing frequencies of 230.538GHz and 345.789GHz, are $130''$ and $80''$, respectively. The pointing and tracking accuracy is better than $10''$. The system temperature were about 120K. The medium and variable resolution acousto optical spectrometers have 1501 and 1601 channels, with total bandwidth of 248 MHz and 544 MHz, and equivalent velocity resolution of 0.21 km s^{-1} and 0.29 km s^{-1} , respectively. The beam efficiency B_{eff} is 0.68 and 0.72 at 230 GHz and 345 GHz, respectively. The forward efficiency F_{eff} is 0.93. Line intensities were converted on the main beam scale, using the formula $T_{\text{mb}} = F_{\text{eff}}/B_{\text{eff}} \times T_{\text{A}}^*$.

Mapping observations are centered at RA(J2000)= $00^{\text{h}}25^{\text{m}}22.7^{\text{s}}$, DEC(J2000)= $64^{\circ}08'50.44''$ using the On-The-Fly mode, the total mapping area is $14.5' \times 15'$ with a $0.5' \times 0.5'$ grid. The observed data were reduced using the CLASS (Continuum and Line Analysis Single-Disk Software) and GREG (Grenoble Graphic) software.

The 1.4GHz radio continuum emission data were obtained from the NRAO VLA Sky Survey (NVSS; Condon et al. 1998).

3 RESULTS

Fig.1 (Left) shows CO $J = 2 - 1$ MCs distribution around Tycho's SNR. The SNR appear as complete shell on the whole and bright knots in southwest, which was detected by the 1.4 GHz radio continuum emission. Three MCs were clearly identified around Tycho's SNR. Each has been designated alphabetically, cloud A, cloud B, and cloud C. In Fig.1 (Left), cloud A-C are well associated with the 1.4 GHz radio continuum emission of Tycho's SNR. It appears that the cloud A and cloud B are spatially adjacent. Here cloud C is for the first time identified around Tycho. Fig.1 (Right) shows the CO $J = 2 - 1$

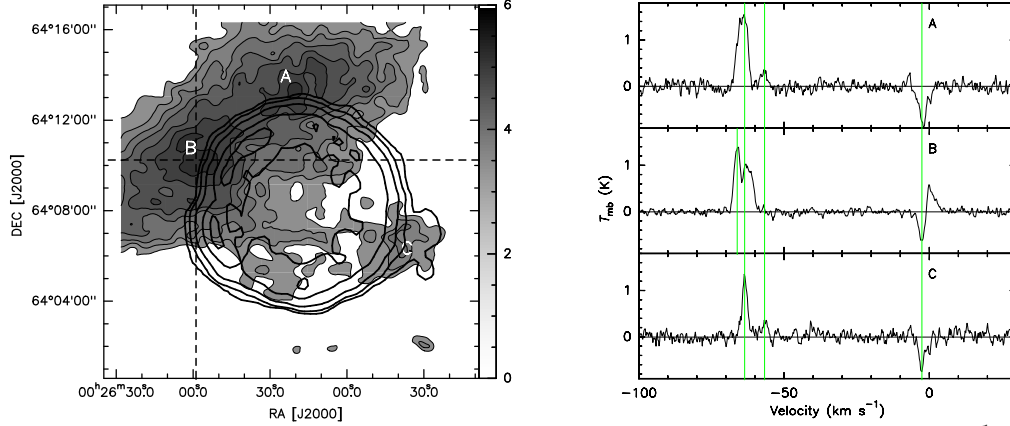


Fig. 1 Left: CO $J = 2 - 1$ intensity map (gray scale) integrated from -69 to -54 km s^{-1} , overlaid on the NVSS 1.4 GHz radio continuum emission contours (black contours). Gray scale levels are from 1.7 to 5.6 K km s^{-1} (the 1σ value is 0.15 K km s^{-1}). Two dashed lines mark the direction of the cuts in Fig.4. Right: Spectra of molecular line CO $J = 2 - 1$ at the peak position of A-C cloud clumps. Letter A, B and C indicate the different MC clumps. The vertical lines in the spectra mark the peak velocity.

spectra towards the peak position of Cloud A-C, respectively. From these spectra, we can see that there are several same velocity components in intervals $-70 \sim -53$ and $-7 \sim 2$ km s^{-1} . The velocity component in interval $-7 \sim 2$ km s^{-1} should belong to the foreground source (Cai et al. 2009). A double-peaked feature is observed in intervals $-70 \sim -53$ for cloud A and cloud B, which can be fitted by Gaussian, respectively. Applying the rotation curve of Clemens (1985) together with $V_0 = 220$ km s^{-1} , where V_0 is the circular rotation speed of the Galaxy, we obtained the distance of Cloud A-C. Tycho's SNR exhibits a complete shell structure of about $8'$. In view of the morphological correspondence of Tycho's SNR and the Cloud A-C, the tangent point (the center of the SNR) in the direction to the SNR is at ~ 4.9 kpc, which is rather close to the distance 4.6 ± 0.5 kpc obtained from the neutral HI absorption observation (Schwarz et al. 1995). The fitted and derived parameters for Cloud A-C are summarized in Table 1. In Table 1, the clouds have broad emission lines. For cloud A, the distance of component peaked at -56.8 km s^{-1} is 4.4 kpc, which is smaller than that of Tycho's SNR (~ 4.9 kpc), so this velocity component can be related to foreground Galactic gas emission. Other components in intervals $-70 \sim -53$ will be analyzed below in relation with Tycho's SNR.

Table 1 The spectral line parameters at the peak positions of clouds

| Name | RA (h m s) | DEC ($^{\circ}$ $'$ $''$) | T_{mb} (rms) (K) | FW (rms) (km s^{-1}) | V_{LSR} (rms) (km s^{-1}) | I (rms) (K km s^{-1}) | Distance (kpc) |
|---------|---------------|--------------------------------|------------------------------|------------------------------------|--|-------------------------------------|-------------------|
| Cloud A | 00 25 20.7 | 64 13 20.44 | 1.6(0.2) | 9.7(0.2) | -63.7(0.1) | 6.7(0.2) | 4.9 |
| | 00 25 20.7 | 64 13 20.44 | 0.4(0.2) | 6.6(0.5) | -56.8(0.2) | 1.0(0.2) | 4.4 |
| Cloud B | 00 25 38.7 | 64 10 20.44 | 1.1(0.1) | 9.7(0.3) | -63.5(0.1) | 4.5(0.2) | 4.9 |
| | 00 25 38.7 | 64 10 20.44 | 1.2(0.1) | 6.3(0.1) | -66.2(0.1) | 3.1(0.3) | 5.0 |
| Cloud C | 00 25 02.7 | 64 06 20.44 | 1.3(0.2) | 7.0(0.1) | -63.6(0.1) | 3.0(0.1) | 4.9 |

The present high- J transition observations enable us to map in detail the molecular gas toward Tycho's SNR. After a careful inspection of the CO component in intervals $-70 \sim -53$, we find that the only channel map can show the morphological and kinematical possible signatures of interaction between Tycho's SNR and the surrounding MCs. Fig.2 shows CO $J = 2 - 1$ intensity channel maps

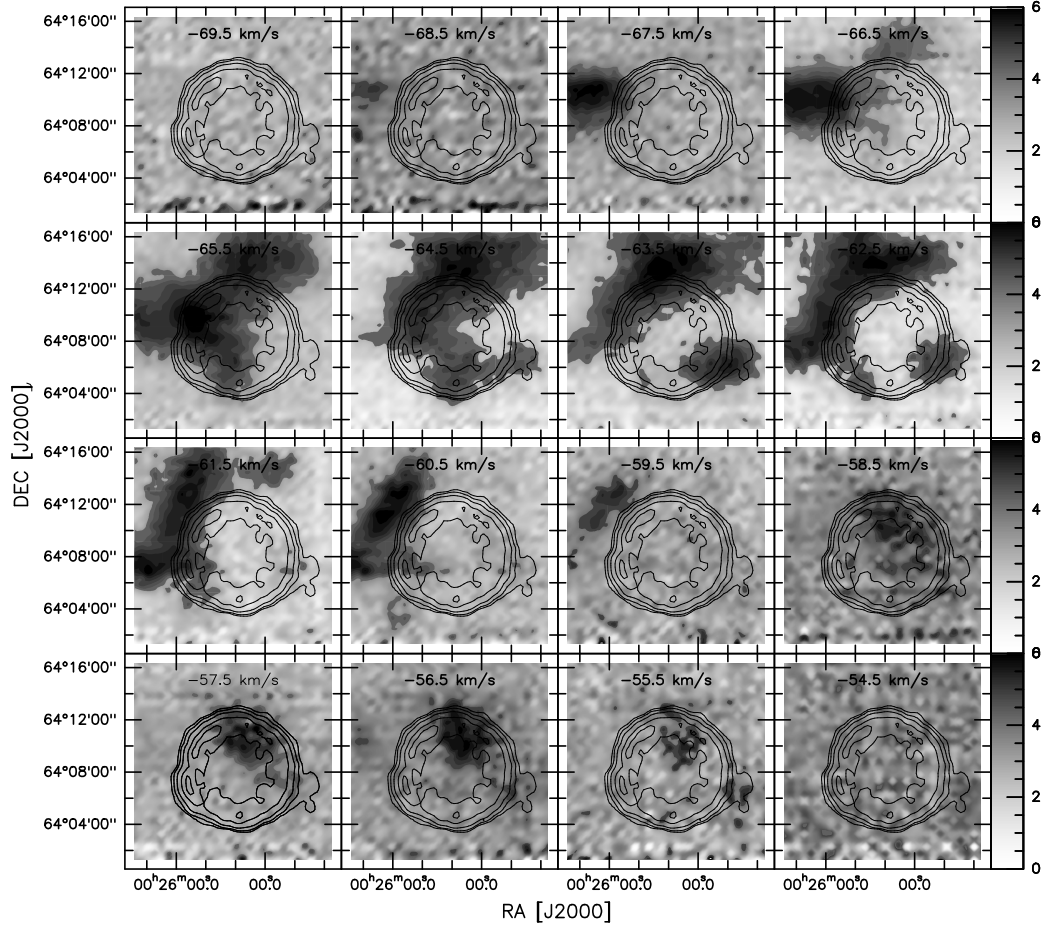


Fig. 2 CO $J = 2 - 1$ channel maps each 1 km s^{-1} , overlapping the NVSS 1.4 GHz radio continuum emission. The radio continuum emission is indicated as black contours. Central velocities are indicated in each image.

over the velocity range of $-70 \sim -53 \text{ km s}^{-1}$ with interval 1 km s^{-1} . The radio continuum emission is indicated as black contours. There is virtually no CO $J = 2 - 1$ emission at $V_{\text{LSR}} > -54 \text{ km s}^{-1}$ and $V_{\text{LSR}} < -69 \text{ km s}^{-1}$, most of the emission is between -69 km s^{-1} and -59 km s^{-1} . In addition, cloud A position has some faint emission in intervals $-59 \sim -54 \text{ km s}^{-1}$. The faint emission corresponds to a CO component peaked at -56.8 km s^{-1} , as seen from the CO $J = 2 - 1$ spectra of cloud A in Fig. 1(Right), which can be related to foreground Galactic gas emission from above analysis. Furthermore, cloud A position have some strong emission in intervals $-67 \sim -59 \text{ km s}^{-1}$, which can be related to a CO component peaked at -63.7 km s^{-1} . This component showing an arc of molecular gas is striking coincident along the northeast boundary. In Fig. 2, there are two velocity components in the intervals $-69 \sim -64$ and $-67 \sim -59 \text{ km s}^{-1}$ for cloud B, corresponding to peak at -66.2 km s^{-1} and -63.5 km s^{-1} in spectra (see Fig. 1). CO $J = 2 - 1$ component at $-69 \sim -64 \text{ km s}^{-1}$ appear to be in contact with the remnant along its eastern boundary. In addition, we can clearly see that the southwest CO $J = 2 - 1$ molecular gas at $-65 \sim -61 \text{ km s}^{-1}$ corresponds to cloud C.

The different transitions of CO trace different molecular environment. In order to obtain the integrated intensity ratio of CO $J = 3 - 2$ and $J = 2 - 1$ ($I_{\text{CO } J=3-2}/I_{\text{CO } J=2-1}$), we convolved the $80''$ of

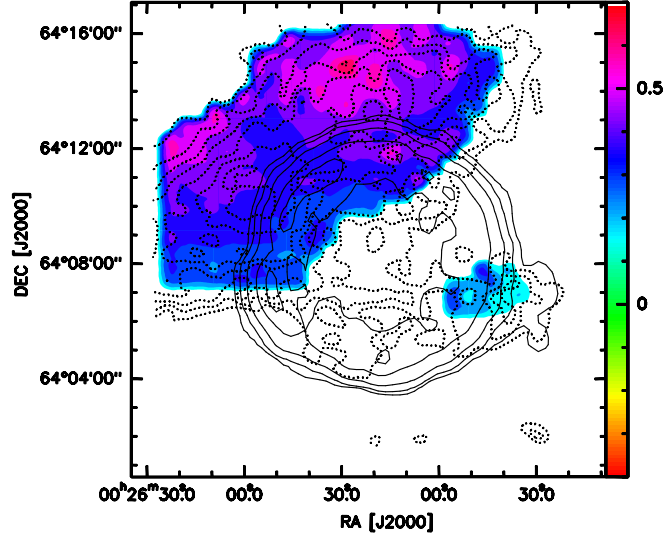


Fig. 3 CO $J = 2 - 1$ intensity map (dashed line) are superimposed on the line intensity ratio map (color scale), the line intensity ratios ($I_{CO J=3-2}/I_{CO J=2-1}$) range from 0.13 to 0.66 by 0.06. The rms level is 0.10 (1σ). The wedge indicates the line intensity ratios scale. Black contours indicate the NVSS 1.4 GHz radio continuum emission.

CO $J = 3 - 2$ data with an effective beam size of $\sqrt{130^2 - 80^2} = 102''$ (Qin et al. 2008). The integrated intensities were calculated for CO $J = 2 - 1$ line in the same velocity range as for CO $J = 3 - 2$. The integrated range is from -69 to -54 km s^{-1} . The rms noise level is 0.15 K km s^{-1} (1σ). Fig.3 shows the distribution of the ratio (color scale) overlaid with the distribution of the CO $J = 2 - 1$ line integrated intensity (black dashed contours); The radio continuum emission is indicated as black contours. The ratio values for the cloud A, cloud B, and cloud C are between 0.23 and 0.66. The rms level is 0.10 (1σ). The maximum value for the three MCs is 0.66, which is in agreement with the value measured in the Milky Way (0.55 ± 0.08 ; Sanders et al. 1993), in NGC 253 (0.5 ± 0.1 in the disk; Wall et al. 1991), and in M33 (0.69 ± 0.15 ; Wilson et al. 1997). It also appear near value measured in the starburst galaxies M82 (0.8 ± 0.2 ; Güsten et al. 1993). In Fig.3, the high ratios (red color) are showed in the northeast part of cloud A and B. The ratio value in this region is greater that in the region where cloud overlaps with Tycho' SNR. The clouds have a ratio value gradient increasing from southwest to northeast, suggesting that SNR shock is expanding into cloud A and B, and start to compress the clouds.

Assuming local thermodynamical equilibrium (LTE) for the gas and optically thick condition for CO $J = 2 - 1$ line, we use the relation $N_{\text{H}_2} \approx 10^4 N_{\text{CO}}$ (Dickman 1978). The column density is estimated as (Garden et al. 1991)

$$N_{\text{CO}} = 6.9 \times 10^{14} \frac{T_{\text{ex}} + 0.92}{\exp(-11.1/T_{\text{ex}})} \int T_{\text{mb}} dv \text{ cm}^{-2}, \quad (1)$$

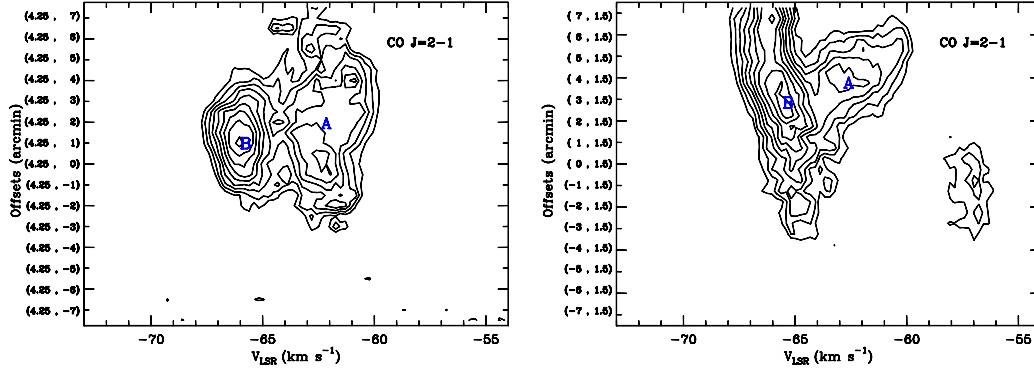
The excitation temperature (T_{ex}) of the CO $J = 2 - 1$ line is estimated following the equation $T_{\text{ex}} = 11.1/\ln[1 + 1/(T_{\text{mb}}/11.1 + 0.02)]$, where T_{mb} is the corrected main beam temperature. Furthermore, their mass is given by $M = \mu N_{\text{H}_2} S / (2.0 \times 10^{33})$, where the mean atomic weight of the gas μ is 1.36, S is the size of core region. The physical parameters of the core are summarized in Table 2.

4 DISCUSSION

Tycho's SNR has complete radio shell on the whole and bright radio knots in southwest. Among the MCs surrounding Tycho's SNR, we have seen that three clouds (cloud A, cloud B and cloud C) are

Table 2 The physical parameters of the core in LTE.

| Name | R (pc) | $T_{\text{ex}}(\text{K})$ | $N_{\text{CO}}(\text{cm}^{-2})$ | $N_{\text{H}_2}(\text{cm}^{-2})$ | $M(M_{\odot})$ |
|---------|--------|---------------------------|---------------------------------|----------------------------------|----------------|
| Cloud A | 5.1 | 5.7 | 2.2×10^{17} | 2.2×10^{21} | 1151 |
| | 1.4 | 3.8 | 0.6×10^{17} | 0.6×10^{21} | 25 |
| Cloud B | 2.8 | 5.0 | 1.7×10^{17} | 1.7×10^{21} | 275 |
| | 5.0 | 5.1 | 1.1×10^{17} | 1.1×10^{21} | 581 |
| Cloud C | 2.1 | 5.3 | 1.1×10^{17} | 1.1×10^{21} | 96 |

**Fig. 4** P-V diagram constructed from the CO $J = 2 - 1$ transition for Cloud B. Left panel: Contour levels are from 0.3 K to 4.4 K by the 0.1 K, with a cut along the north-south direction. Right panel: Contour levels are the same as in left panel, with a cut along the east-west direction.

spatially coincident with the SNR. Broad emission lines detected in cloud A and B and bow-shaped morphology suggest that the MCs may be interacting with the SNR. After a careful inspection of the CO component, we find that CO component of cloud A in intervals $-67 \sim -59 \text{ km s}^{-1}$ (peaked at -63.7 km s^{-1}) and CO component of cloud B in intervals $-69 \sim -64 \text{ km s}^{-1}$ (-66.2 km s^{-1}) and $-67 \sim -59 \text{ km s}^{-1}$ (-63.5 km s^{-1}) are well associated with Tycho's SNR. The position-velocity diagram across the peak of cloud B along the north-south and the east-west direction, respectively, are constructed from the CO $J = 2 - 1$ line (see Fig.4). In Figure 4, obviously, the velocity components of cloud A and cloud B are adjacent. For cloud A, CO component in intervals $-67 \sim -59 \text{ km s}^{-1}$ may belong to cloud B, because cloud A and cloud B are adjacent in space and in velocity, and have the approximately same peak velocity in spectra. We concluded that cloud A and cloud B may not only simply be overlapping along the line of the sight, but also colliding each other. Furthermore, the new cloud C is also associated well with bright knots, the bright knots may be radio emissivity increase due to compression of the shocked material, suggesting that cloud C appears to be swept up by the SNR shock in the southwest area.

The maximum value of integrated CO line intensity ratio for the three MCs is 0.66 ± 0.10 . The comparison with previously published observations reveals that the $I_{\text{CO},J=3-2}/I_{\text{CO},J=2-1}$ for the MCs associated with Tycho's SNR agrees well with the value measured in in the Milky Way (0.55 ± 0.08 ; Sanders et al. 1993), in NGC 253 (0.5 ± 0.1 in the disk; Wall et al. 1991), and in M33 (0.69 ± 0.15 ; Wilson et al. 1997). It also appear near value measured in the starburst galaxies M82 (0.8 ± 0.2 ; Güsten et al. 1993). The high $I_{\text{CO},J=3-2}/I_{\text{CO},J=2-1}$ in starburst galaxies may be due to unusual conditions in these dense and hot regions (Aalto et al. 1997), while for normal MCs the most likely explanation is a significant contribution to the CO emission by low column density material (Wilson & Walker 1994). Moreover, the high $I_{\text{CO},J=3-2}/I_{\text{CO},J=2-1}$ value (3.4) in the MCs interacting with SNR IC443 (Xu et

al. 2010) exceed previous measurement of individual Galactic MCs, implying that the SNR shock has driven into the MCs. For the MCs around Tycho's SNR, the $I_{\text{CO } J=3-2}/I_{\text{CO } J=2-1}$ value (0.66 ± 0.10) may indicate that the Tycho's SNR shock just drove into the surrounding MCs. In addition, the MCs associated with HII regions have higher ratio of $I_{\text{CO } J=3-2}/I_{\text{CO } J=2-1}$ and have higher gas temperature than those sources without HII regions, indicating that the high line ratio may be due to heating of the gas by the massive stars (Wilson et al. 1997). Different masers maybe occur in different astrophysical environment. The H₂O masers are located near the MSX sources and within the maximum line intensity ratio $I_{\text{CO } J=3-2}/I_{\text{CO } J=2-1}$ regions, suggesting that H₂O masers occur in relatively warm environments (Qin et al. 2008). Thus, we concluded that the line intensity ratios based on the optically thick CO transitions indicate the temperature varies at different positions. The MCs associated with Tycho' SNR have a ratio value gradient increasing from southwest to northeast, may imply that a shock has driven into MCs and compressed MCs. Since the MCs are compressed, it lead to the temperature of molecular gas increases. Hence the line intensity ratio $I_{\text{CO } J=3-2}/I_{\text{CO } J=2-1}$ will increase. We consider that high $I_{\text{CO } J=3-2}/I_{\text{CO } J=2-1}$ is also identified as one good signature of SNR-MCs interaction system. From Table 1, the total mass of MCs is $\sim 2.13 \times 10^3$.

5 SUMMARY

We have presented large-area map of molecular clouds (MCs) in the vicinity of Tycho' SNR in CO $J = 2-1$ and CO $J = 3-2$ lines. The complete map suggests that MCs are mainly distributed along the northern and eastern boundary of the SNR. It also reveals a new cloud (cloud C) that appears to be swept by the SNR shock in the southwestern area. The bow-sharped morphology, the broad emission lines, as well as the integrated CO line intensity ratios ($I_{\text{CO } J=3-2}/I_{\text{CO } J=2-1}$) (0.66 ± 0.10) further suggest that these MCs are interacting with Tycho' SNR. The MCs is revealed at $-69 \sim -59 \text{ km s}^{-1}$, well coincident with the Tycho's SNR. The MCs associated with Tycho's SNR have a mass of $\sim 2.13 \times 10^3 M_{\odot}$. In the northern and eastern MCs, we find a line intensity ratio gradient along the southwest-northeast direction, implying that Tycho' SNR shock has driven into the MCs. We concluded that the line intensity ratios based on the optically thick CO transitions indicate the temperature varies at different positions. Both the integrated intensity maps and position-velocity diagrams show the eastern and northern clouds adjacent in space and velocity. Together with the approximately same peak velocity in spectra, we found that the two MCs are interacting, indicating possible cloud-cloud collision in this region.

Acknowledgements We are very grateful to the anonymous referee for his/her helpful comments and suggestions. This work was supported by the National Natural Science Foundation of China under Grant No.10473014.

References

- Aalto, S., Radford, S. J. E., Scoville, N. Z., & Sargent, A. I. 1997, ApJ, 475, L107
- Albinson, J. F., Tuffs, R. J., Swinbank, E., et al. 1986, MNRAS, 219, 427
- Cai, Z. Y., Yang, J., & Lu, D. R., 2009, Chinese Astronomy and Astrophysics, 33, 393
- Clemens, D. P. 1985, ApJ, 295, 442
- Condon, J. J., Cotton, W. D., Greisen, E. W., et al. 1998, AJ, 115, 1693
- Dickel, J. R., van Breugel, W. J. M., Storm, R. G. 1991, AJ, 101, 2151
- Dickman, R. L. 1978, ApJS, 37, 407
- Garden, R. P., Hayashi, M., Hasegawa, T., Gatley, I., & Kaifu, N. 1991, ApJ, 374, 540
- Güsten, R., Serabyn, E., Kasemann, C., et al. 1993, ApJ, 402, 537
- Hwang, U., Decourchelle, A., Holt, S. S., & Petre, R. 2002, ApJ, 581, 1101
- Jiang, B., Chen, Y., Wang, J. Z., et al. 2010, ApJ, 712, 1147
- Kamper, K. W., & van den Bergh, S. 1978, ApJ, 224, 851
- Lee, J. J., Koo, B. C., & Tatsumatsu, Keni'chi. 2004, ApJ, 605, L113
- Qin, S. L., Wang, J. J., Zhao, G., Miller, M., & Zhao, J. H. 2008, A&A, 484, 361

- Reynoso, E. M., Moffett, D. A., Goss, W. M., et al., 1997, *ApJ*, 491, 816
Reynoso, E. M., Velázquez, P. F., Dubner, G. M., & Goss, W. M. 1999, *AJ*, 117, 1827
Reynoso E. M., & Mangum J. G. 2000, *ApJ*, 545, 874
Reynoso, E. M., & Mangum, J. G. 2001, *AJ*, 121, 347
Sanders, D. B., Scoville, N. Z., Tilanus, R. P. J., et al. 1993, in *Back to the Galaxy*, ed. S. S. Holt & F. Verter (New York: AIP), 311-121, 347
Schwarz, U. J., Goss, W. M., Kalberla, P. M., & Benaglia, P. 1995, *A&A*, 299, 193
Strom, R. G. 1988, *MNRAS*, 230, 331
Wall, W. F., Jaffe, D. T., Bash, F. N., & Israel, F. P. 1991, *ApJ*, 380, 384
Wilson, C. D., & Walker, C. E. 1994, *ApJ*, 432, 148
Wilson, C. D., Walker, C. E., & Thornley, M. D. 1997, *ApJ*, 483, 210
Xu, J. L., Wang, J. J., & Miller, M. 2010, arXiv:1011.3652